Remote Sensing Reflectance and Derived Ocean Color Products from MODIS to VIIRS

Bryan Franz

Ocean Ecology Laboratory
NASA Goddard Space Flight Center

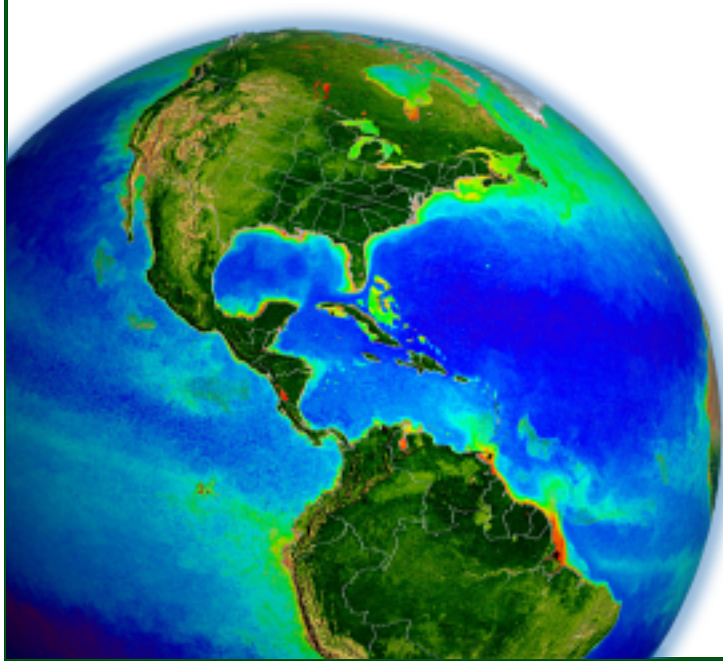

MODIS Science Team Meeting

19-22 May 2015, Silver Spring, MD

Proposal Team: MODIS & VIIRS

Team Member	**Primary Role**
Bryan Franz	project lead & quality assessment
Zia Ahmad	atmospheric correction
Sean Bailey	vicarious calibration & software
Gene Eplee	VIIRS calibration
Gerhard Meister	MODIS calibration
Chris Proctor	in situ validation
Kevin Turpie	VIIRS prelaunch
Jeremy Werdell	bio-optical algorithms

and the Ocean Biology Processing Group ...

2014.0 Multi-Mission Ocean Reprocessing

Scope

- OC from CZCS, OCTS, SeaWiFS, MERIS, MODIS(A/T), and VIIRS
- SST from MODIS

Motivation

1. improve interoperability and sustainability of the product suite by adopting modern data formats, standards, and conventions
2. incorporate algorithm updates and advances from community and last MODIS Science Team developed since 2010 (last algorithm change)
3. incorporate knowledge gained in instrument-specific radiometric calibration and updates to vicarious calibration

Status

- OC from OCTS & **VIIRS done, MODISA in progress**
- SST from MODISA and MODIST done (not yet released)

Remote Sensing Reflectance (Rrs; sr^{-1})

Rrs is the ratio of upwelling "water-leaving" radiance to downwelling irradiance, just above the sea surface

Rrs is the fundamental remote sensing quantity from which most ocean color products are derived (e.g., chlorophyll, particulate organic and inorganic carbon, inherent optical properties)

Atmospheric Correction

observed TOA
Rayleigh
aerosol + Ray-aer
foam & whitecaps
Sun glint
water-leaving

$$L_t = \left(L_r + \left[L_a + L_{ra}\right] + t_{dv} L_f + T_s T_v L_g + t_{dv} L_w\right) t_{gv}\, t_{gs}\, f_p$$

$$R_{rs} = \frac{L_w}{F_0 \cos(\theta_s)\, t_{ds}\, f_s} f_b\, f_\lambda$$

$$nL_w = F_0 R_{rs}$$

adaptation to VIIRS

- algorithm modifications limited to adjustment for sensor-specific spectral band centers and relative spectral responses

- same Ahmad-Fraser vector radiative transfer code used to derive MODIS & VIIRS-specific Rayleigh and aerosol model tables

- bands used for aerosol determination

MODIS:	748 & 869 nm
VIIRS:	745 & 862 nm

Rrs(λ) for Spring 2012

MODISA 443 nm

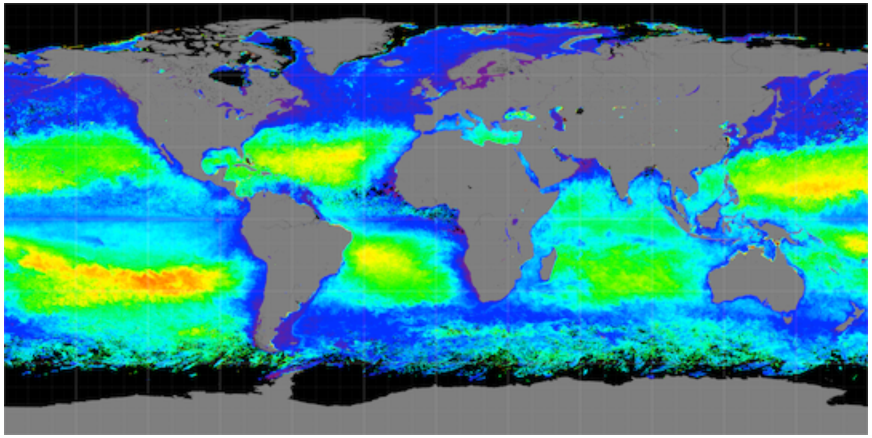

MODISA 547 nm

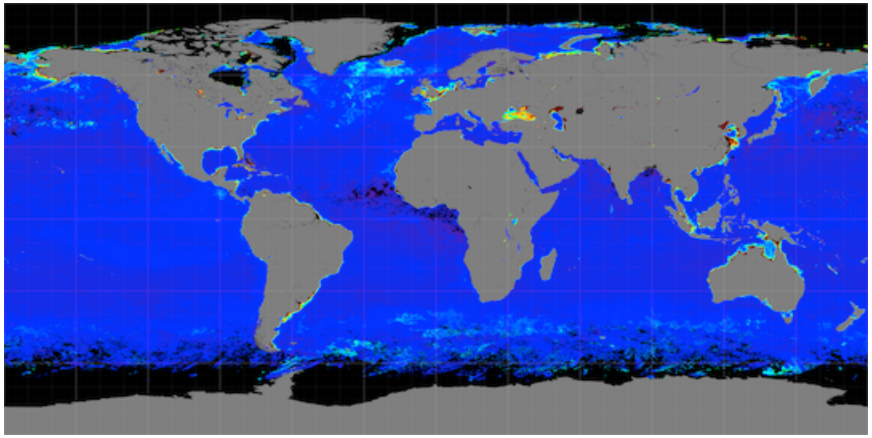

VIIRS 443 nm

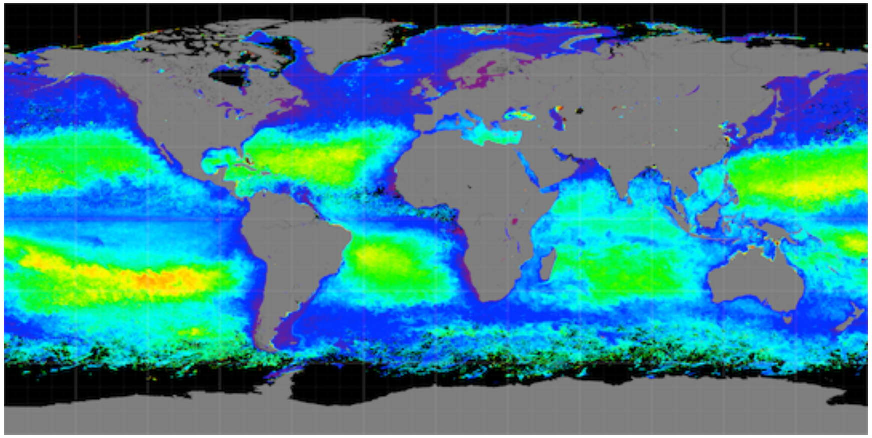

VIIRS 551 nm

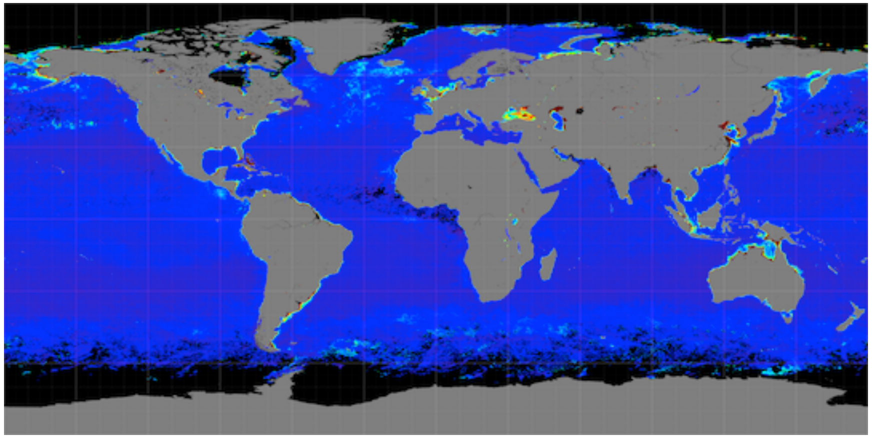

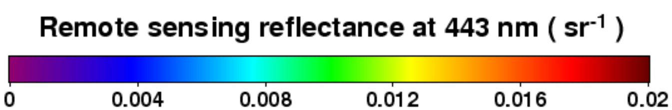

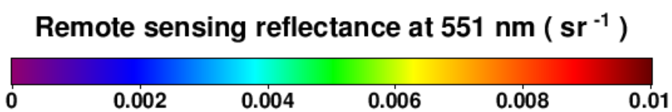

Chl_a for Spring and Fall 2012

MODISA Spring

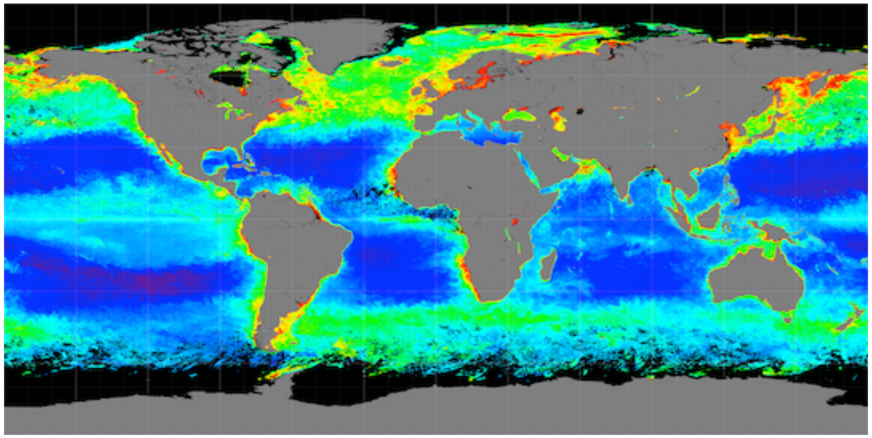

MODISA Fall

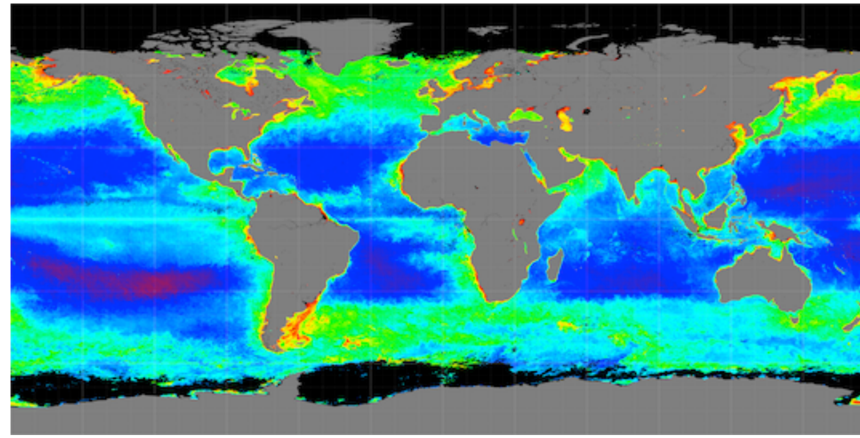

VIIRS Spring

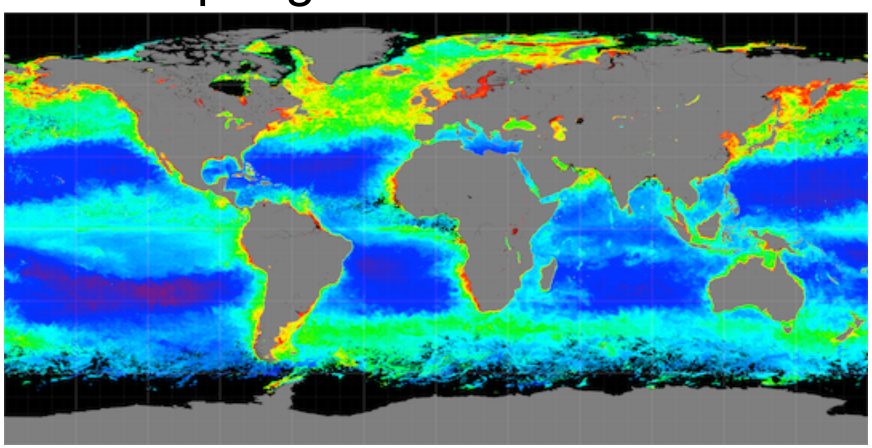

VIIRS Fall

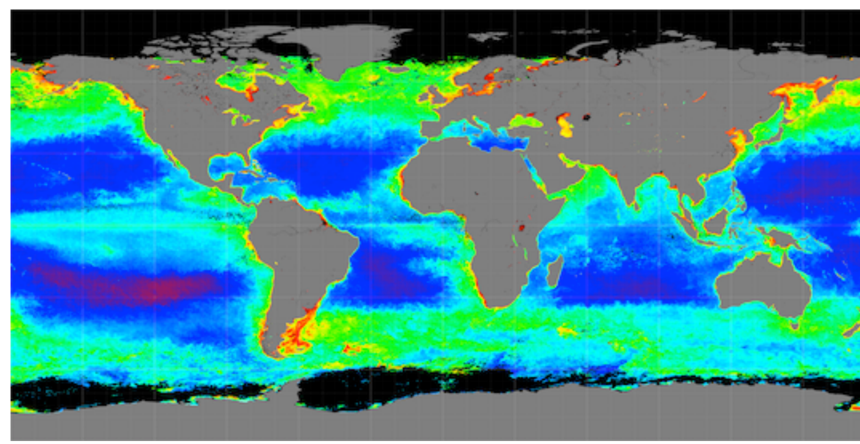

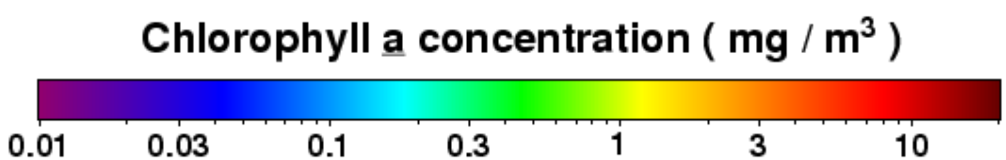

Global Mid-Latitude (+/-

showing suspect tr

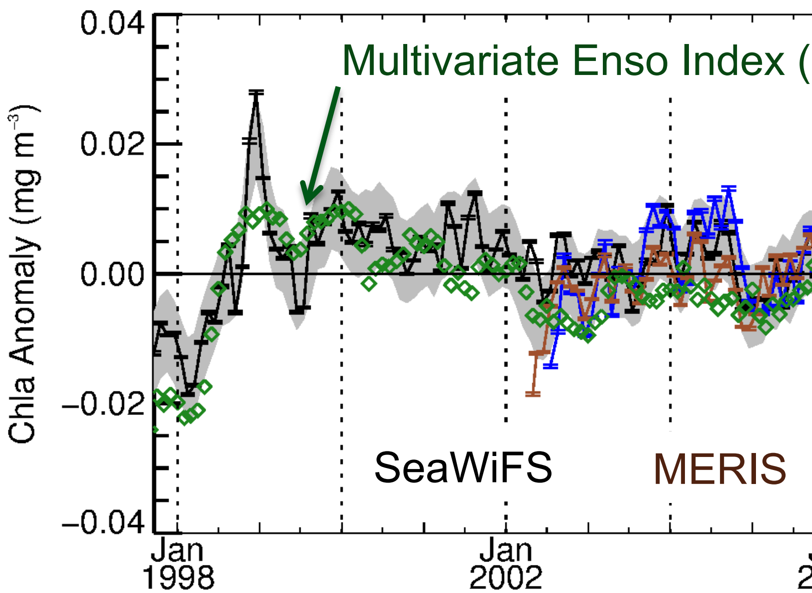

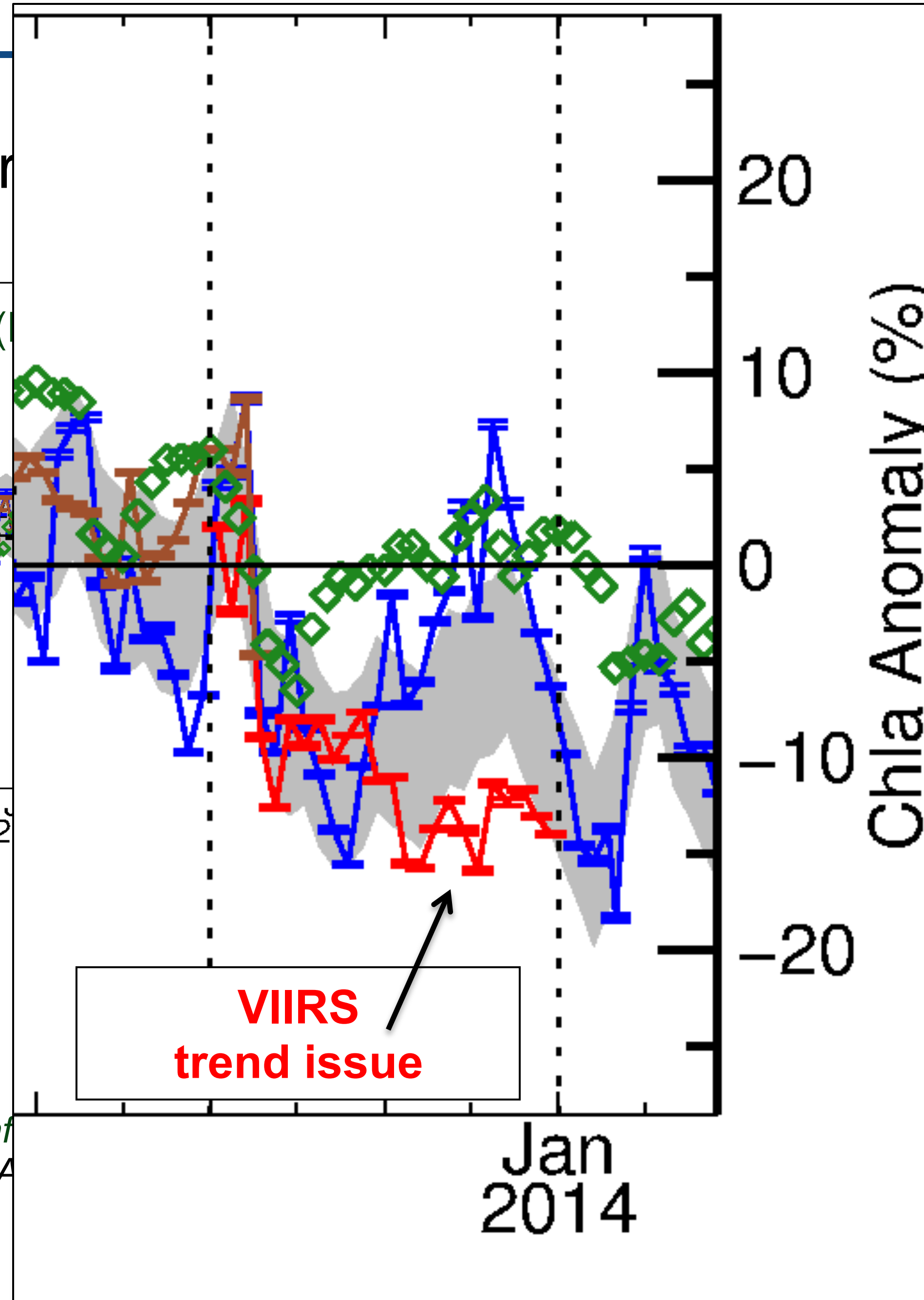

before latest reprocessing

Following *Franz, B.A., D.A. Siegel, M.J. Behrenf*
[in State of the Climate in 2013]. Bulletin of the A

VIIRS R2014.0 calibration

Significantly improved instrument calibration developed for ocean color through re-analysis of VIIRS prelaunch and on-orbit calibration.

1) Based on solar calibration, corrected with lunar calibration.

2) Incorporating advancements in solar and lunar calibrator knowledge (solar diffuser stability, solar unit vector fix, lunar libration corrections, etc.).

3) implemented as a continuous calibration model that allows for extrapolation into the future (improved NRT calibration quality).

4) Including corrections for relative detector and mirror-side calibration to reduce image striping artifacts.

Robert E. Eplee, Kevin R. Turpie, Gerhard Meister, Frederick S. Patt, Bryan A. Franz, and Sean W. Bailey, "On-orbit calibration of the Suomi National Polar-Orbiting Partnership Visible Infrared Imaging Radiometer Suite for ocean color applications," Appl. Opt. 54, 1984-2006 (2015)

VIIRS Reduced Image Striping

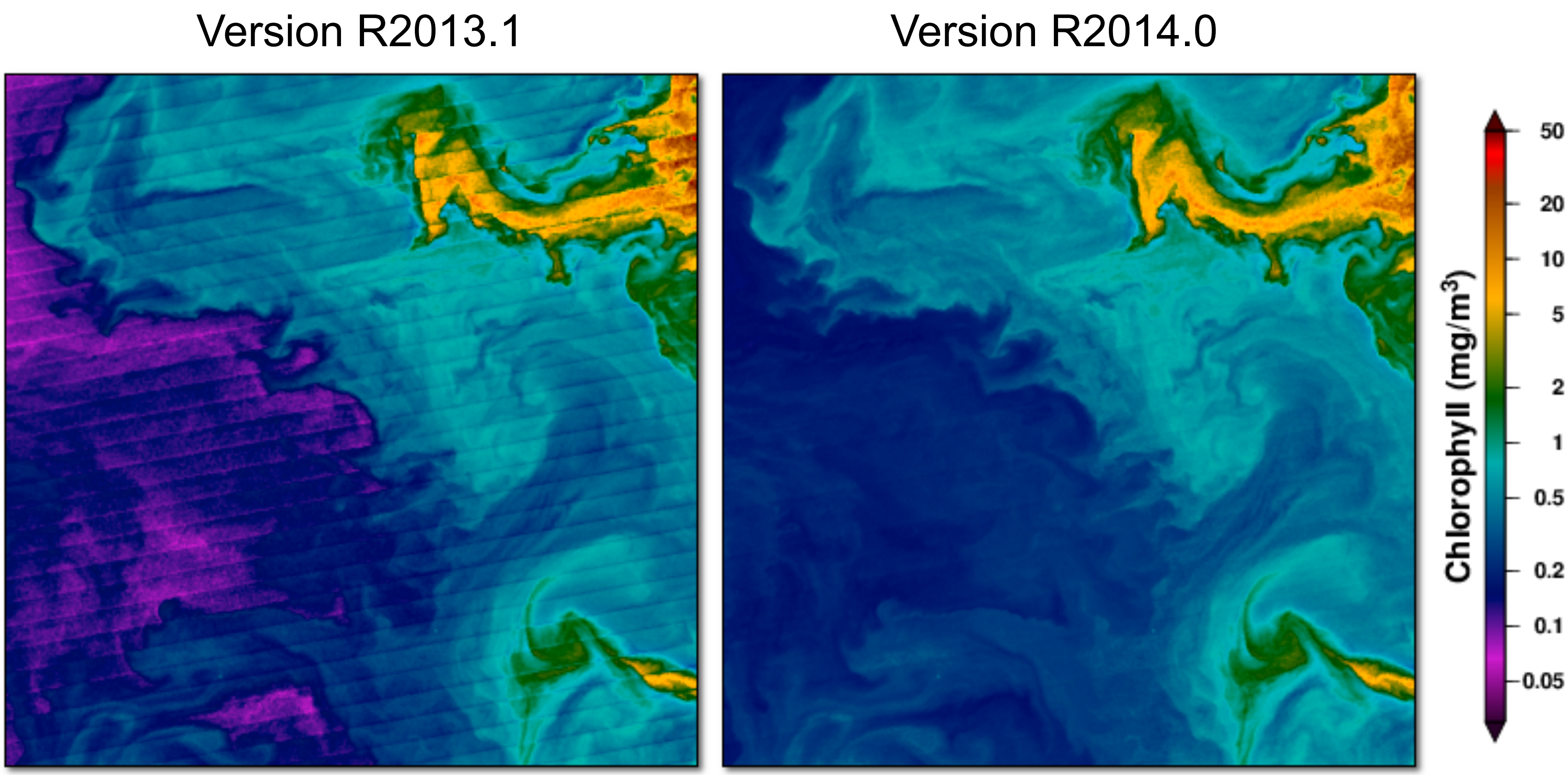

Revised instrument calibration includes detector relative calibration to reduce image striping artifacts.

VIIRS Clear-Water Rrs(λ) Time-Series Comparison

Before & After R2014.0 Reprocessing

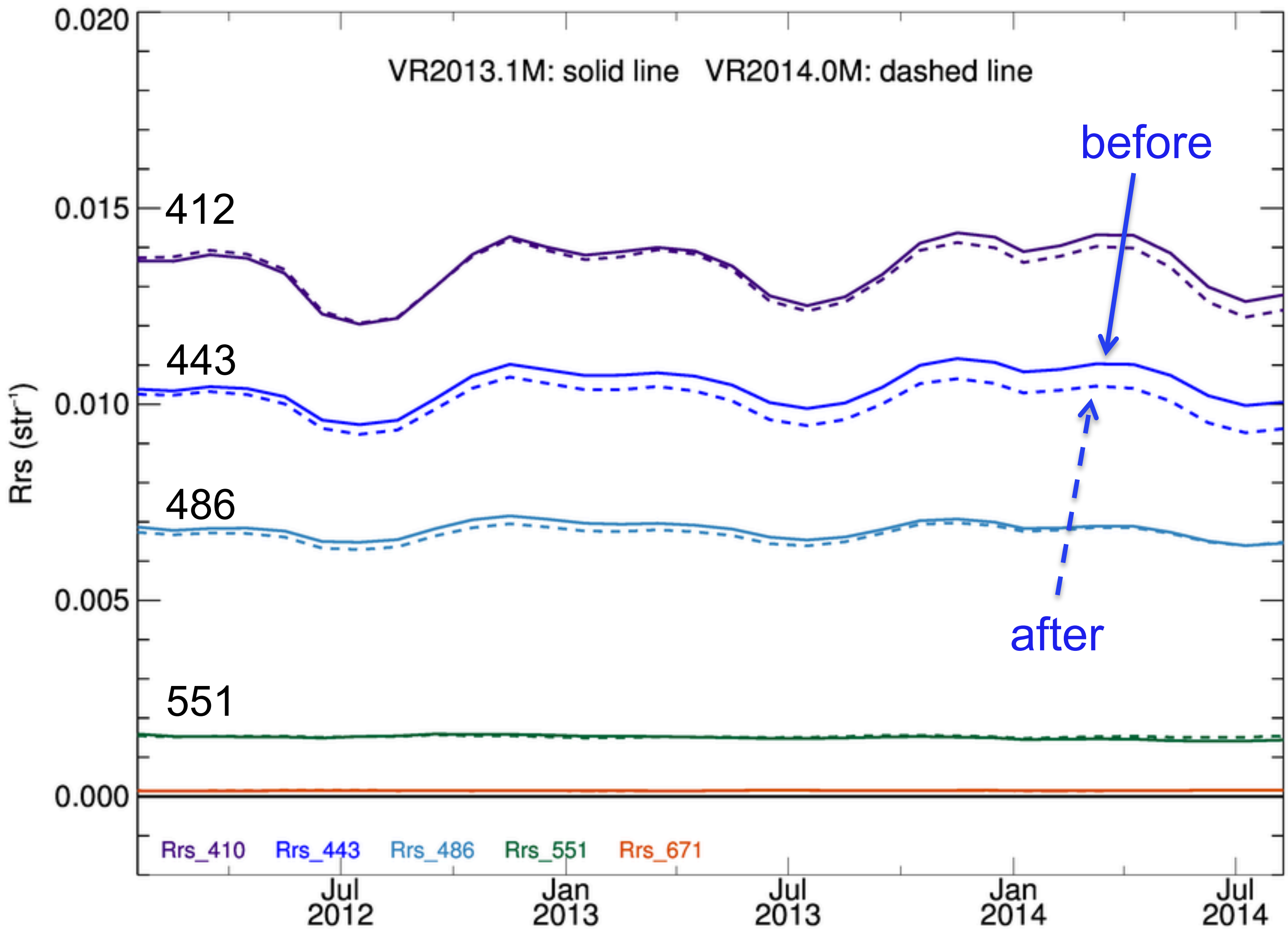

VIIRS Clear-Water Rrs Anomaly Trends

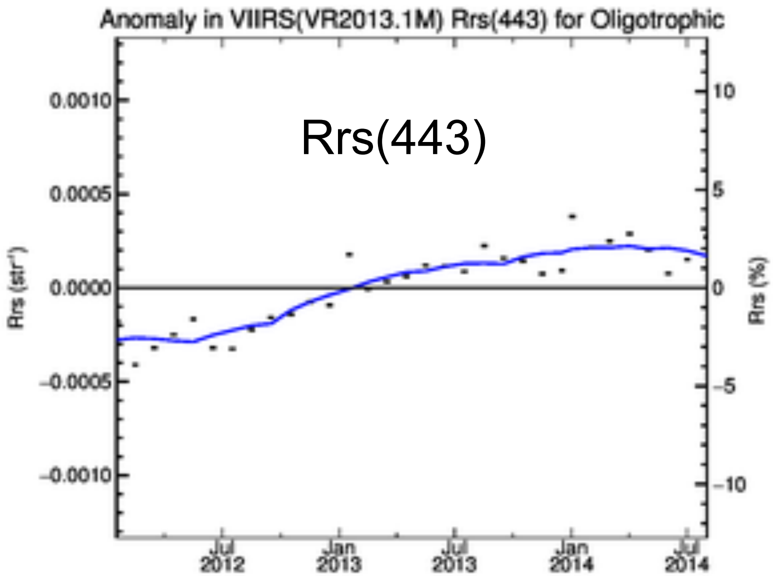

Before Reprocessing R2013.1

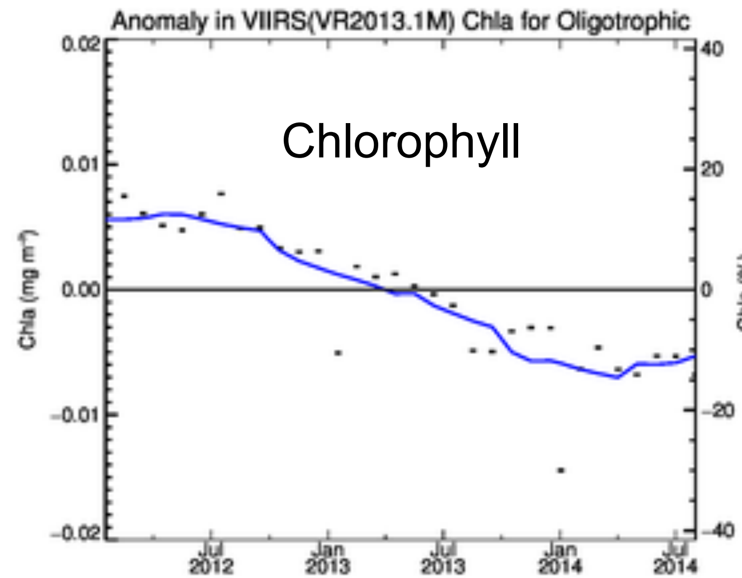

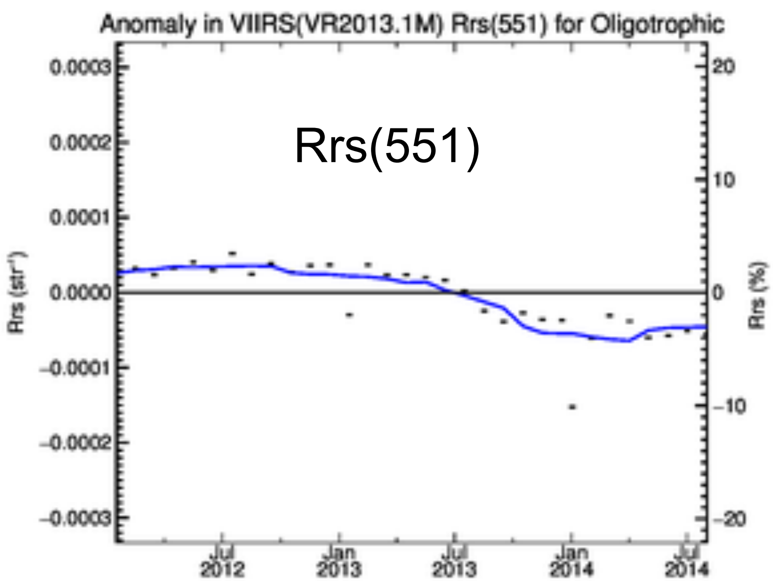

VIIRS Clear-Water Rrs Anomaly Trends

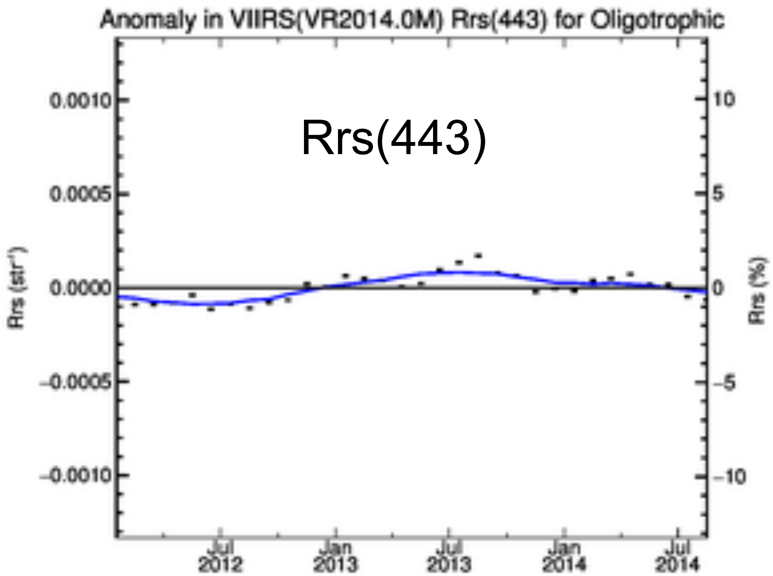

After Reprocessing R2014.0

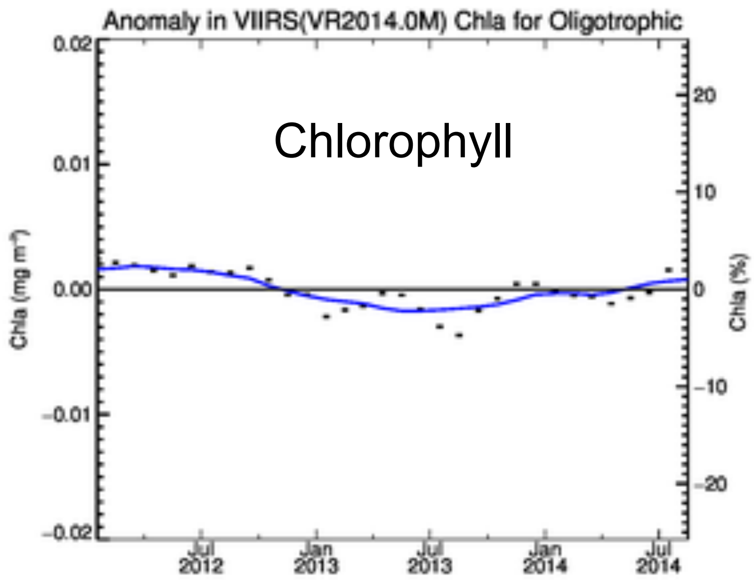

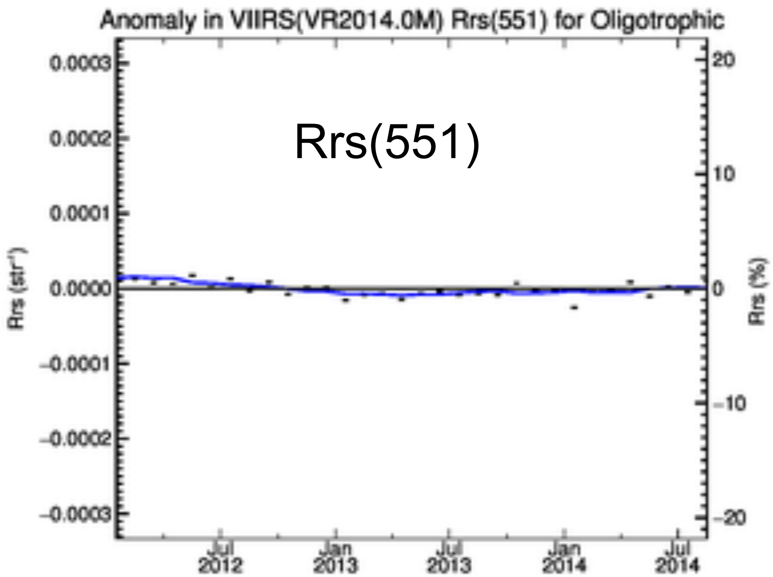

Global Mid-Latitude (+/- 40°) Chlor

showing improved agreement of VIIRS with I
historical norms after R2014.0 repr

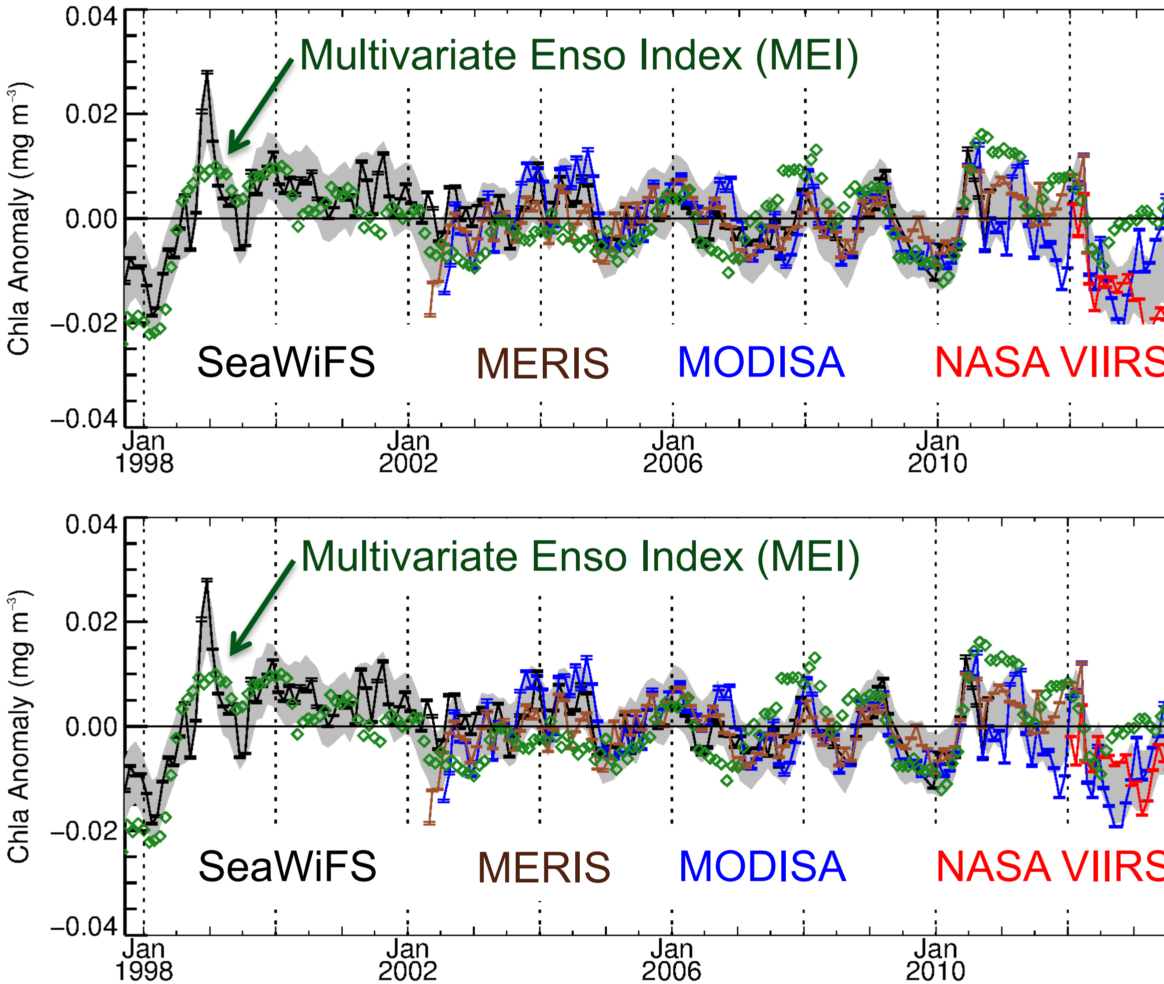

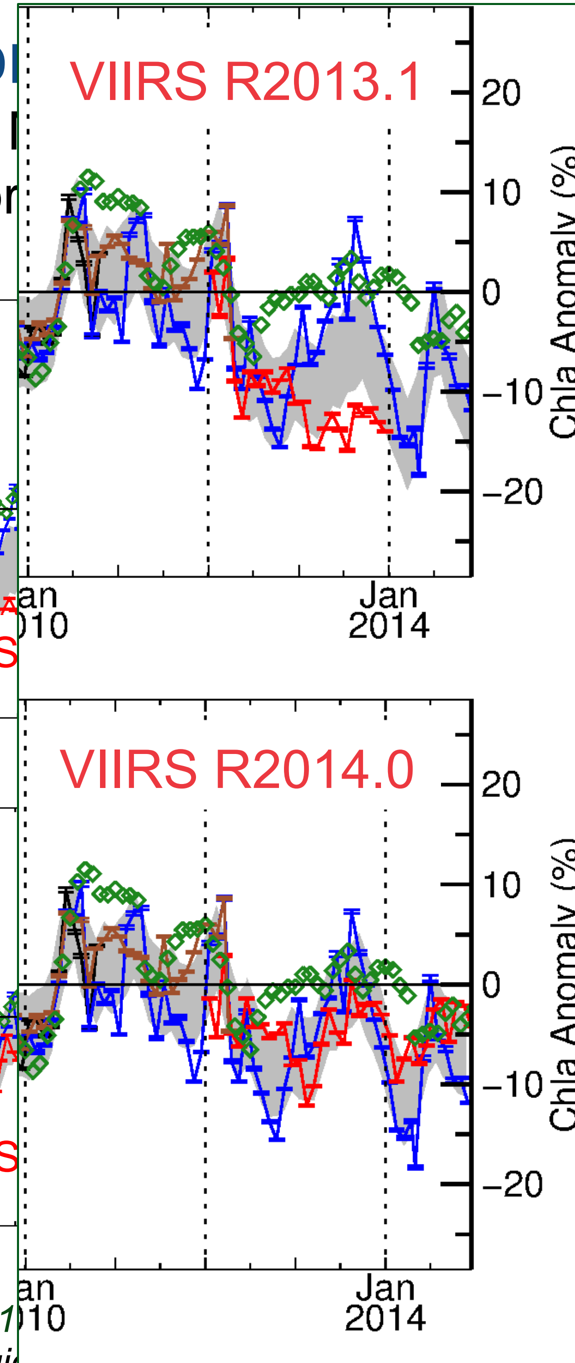

Following *Franz, B.A., D.A. Siegel, M.J. Behrenfeld, P.J. Werdell (201*
[in State of the Climate in 2014]. Bulletin of the American Meteorologi

MODISA Calibration Issues

- Collection 6 calibration and subsequent updates are being applied, but standard calibration may not be sufficient to fully characterize late-mission temporal calibration changes to level required for ocean color.
- MODIS/Aqua Rrs showing increased temporal variability in blue (412, 443) water-leaving reflectance trends after 2011. Is it real?

MODISA Rrs(λ) Deep-Water Time-Series

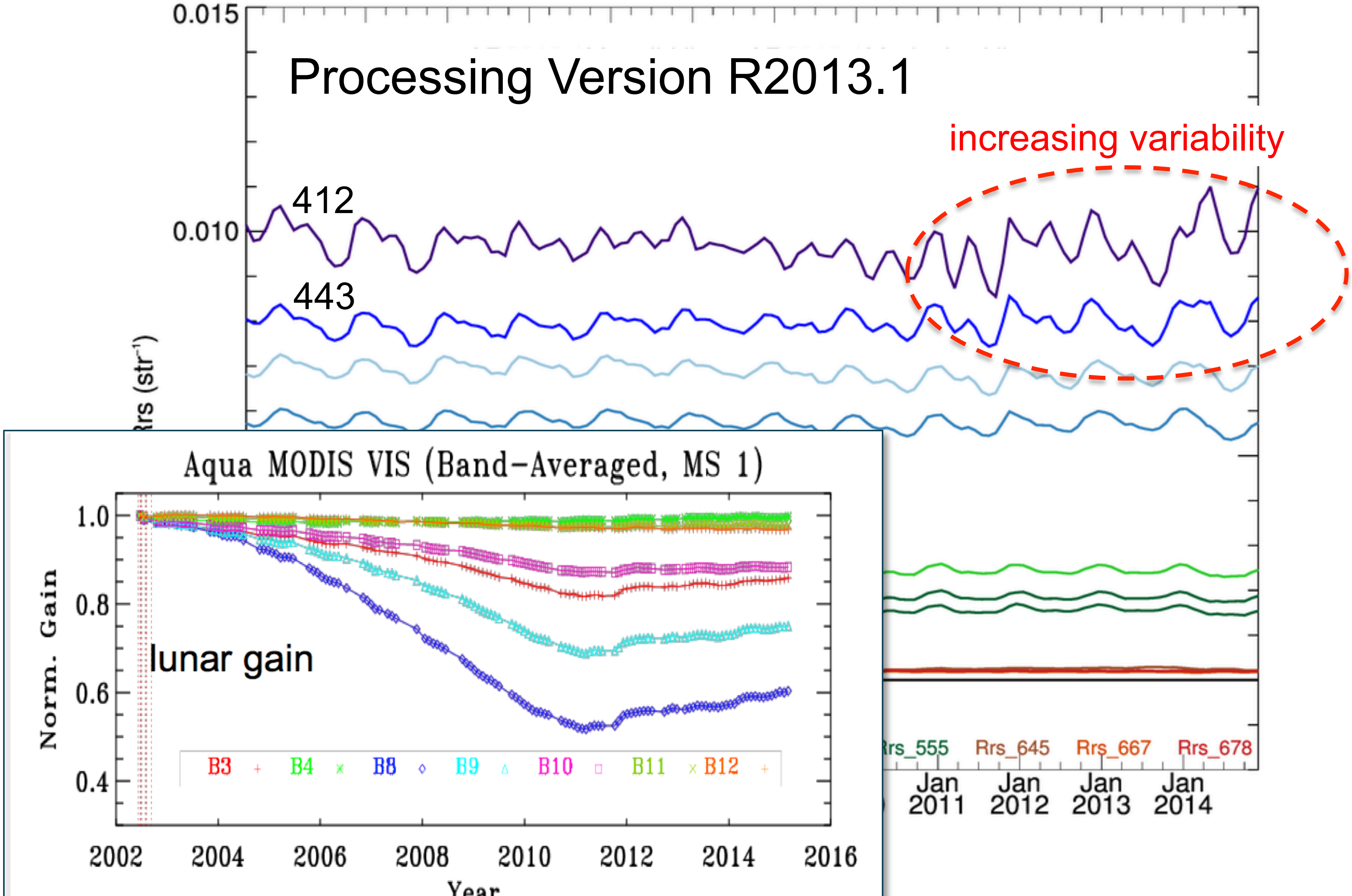

MODIS Calibration Issues

- Collection 6 calibration and subsequent updates are being applied, but standard calibration may not be sufficient to fully characterize late-mission temporal calibration changes to level required for ocean color.
- MODIS/Aqua Rrs showing increased temporal variability in blue (412, 443) water-leaving reflectance trends after 2011. Is it real?
- In 2014, all radiometry shifted (up in blue, down in green), with commensurate decline of 10% in clear-water chlorophyll.

MODISA Clear-Water Rrs Anomaly Trends

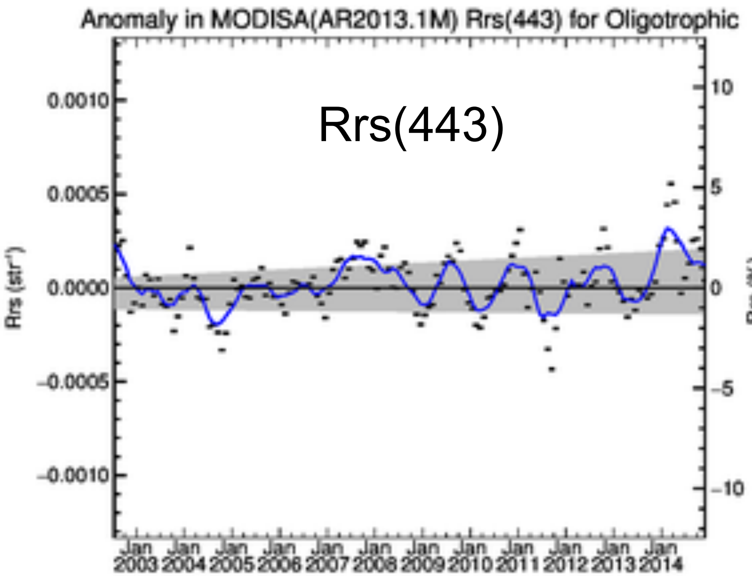

Current Operational
R2013.1

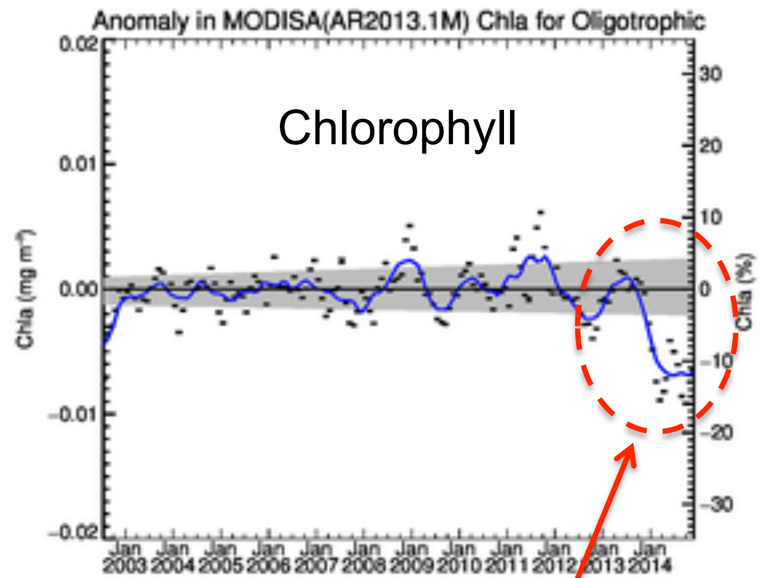

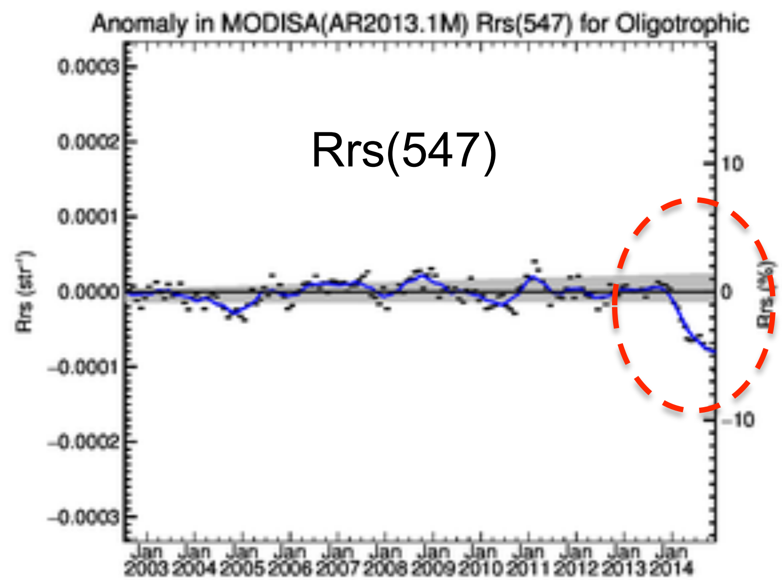

2014 anomaly
"calibration issue"

MODIS Calibration Issues

- Collection 6 calibration and subsequent updates are being applied, but standard calibration may not be sufficient to fully characterize late-mission temporal calibration changes to level required for ocean color.
- MODIS/Aqua Rrs showing increased temporal variability in blue (412, 443) water-leaving reflectance trends after 2011. Is it real?
- In 2014, all radiometry shifted (up in blue, down in green), with commensurate decline of 10% in clear-water chlorophyll.
- Our team and MCST have been working to resolve these issues in preparation for MODISA reprocessing 2014.0, with some success.

MODISA Clear-Water Rrs Anomaly Trends

Reprocessing Test Results

MCST LUT V6.1.33.8_OC2
+ OBPG cross-scan corrections

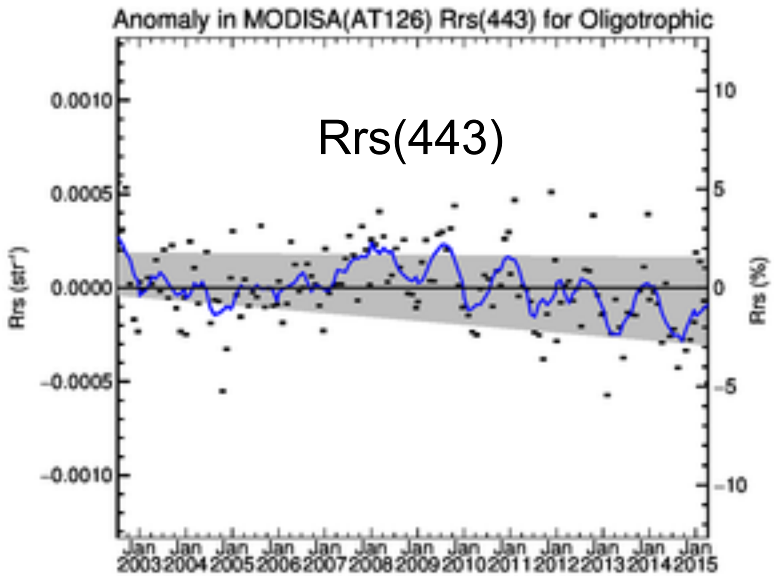

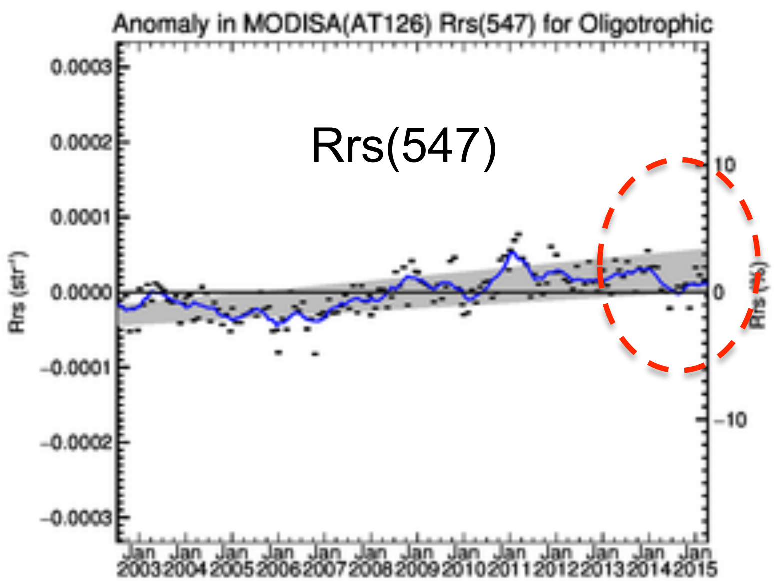

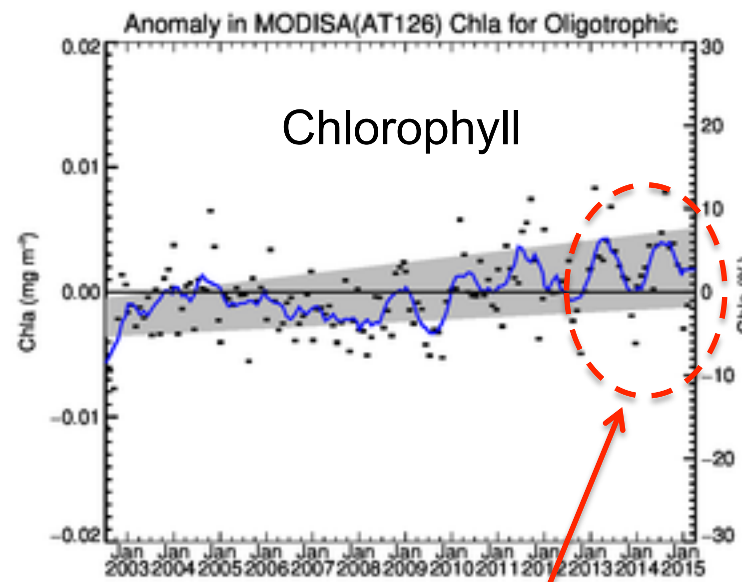

2014 anomaly "resolved"

MODISA & VIIRS Rrs(λ) Clear-Water Time-Series

showing "good" agreement

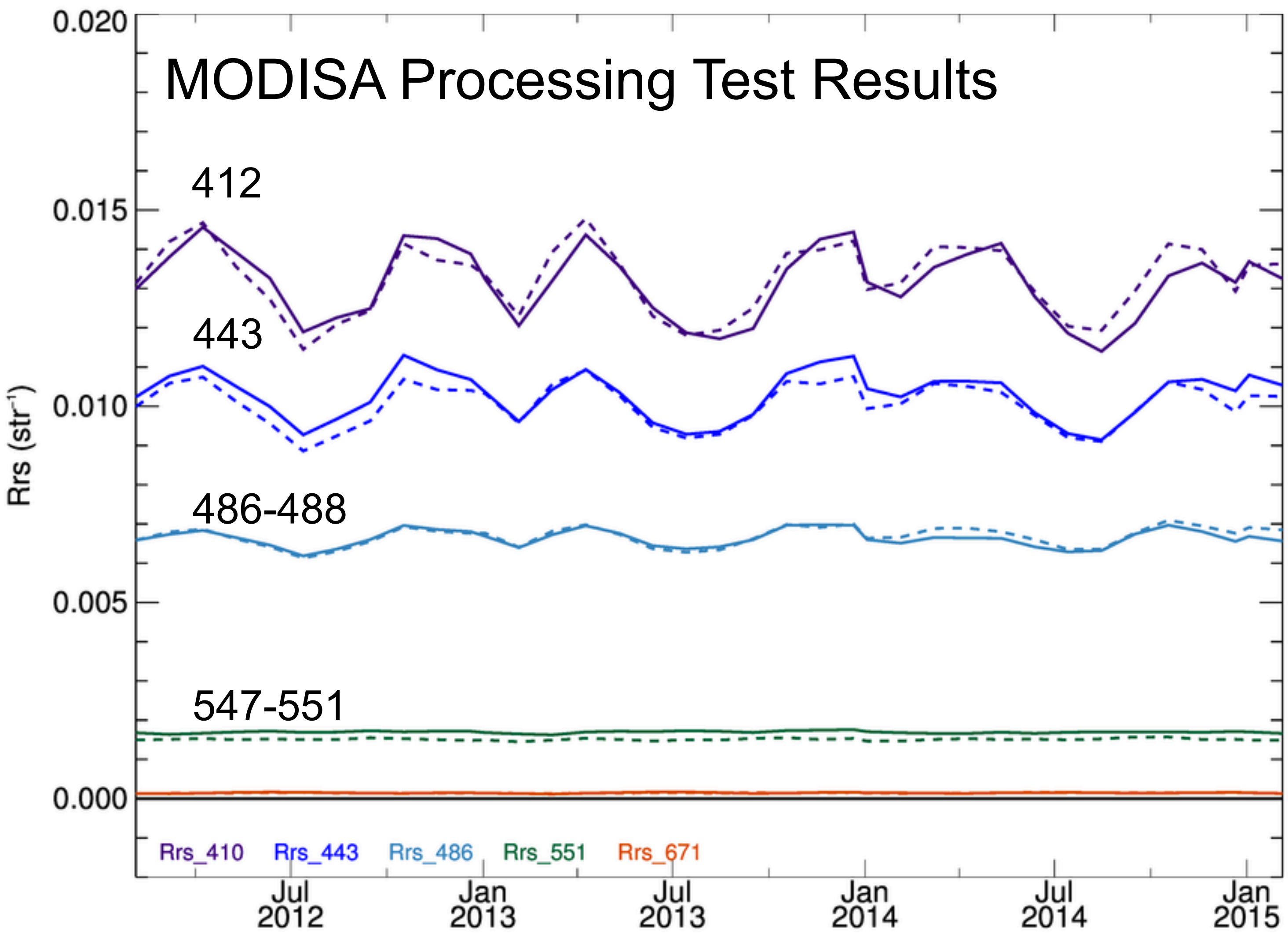

MODISA & VIIRS Rrs(λ) Deep-Water Time-Series

showing “good” agreement

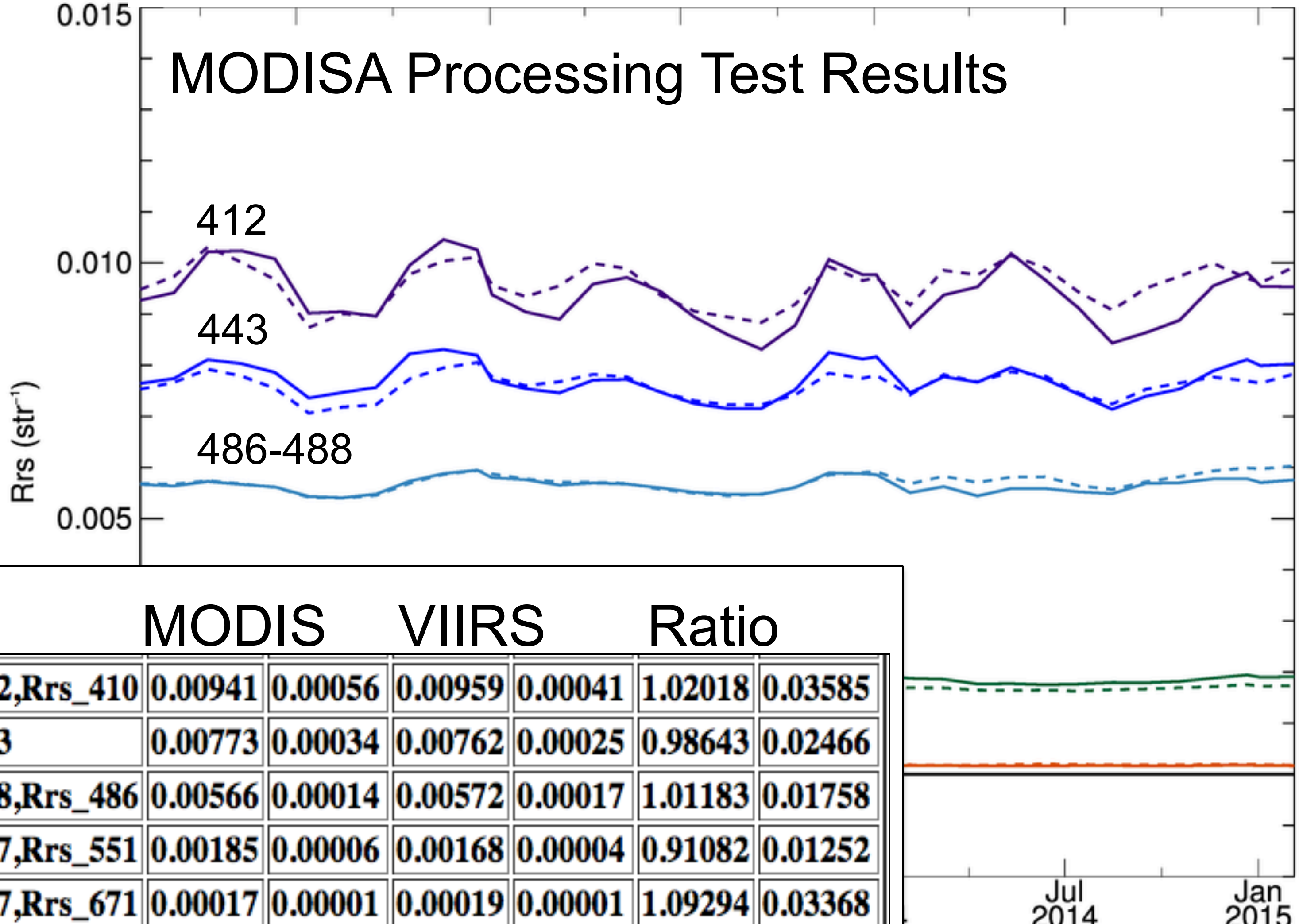

	MODIS		VIIRS		Ratio	
Rrs_412,Rrs_410	0.00941	0.00056	0.00959	0.00041	1.02018	0.03585
Rrs_443	0.00773	0.00034	0.00762	0.00025	0.98643	0.02466
Rrs_488,Rrs_486	0.00566	0.00014	0.00572	0.00017	1.01183	0.01758
Rrs_547,Rrs_551	0.00185	0.00006	0.00168	0.00004	0.91082	0.01252
Rrs_667,Rrs_671	0.00017	0.00001	0.00019	0.00001	1.09294	0.03368

VIIRS R2014.0 In Situ Validation

Rrs(443)

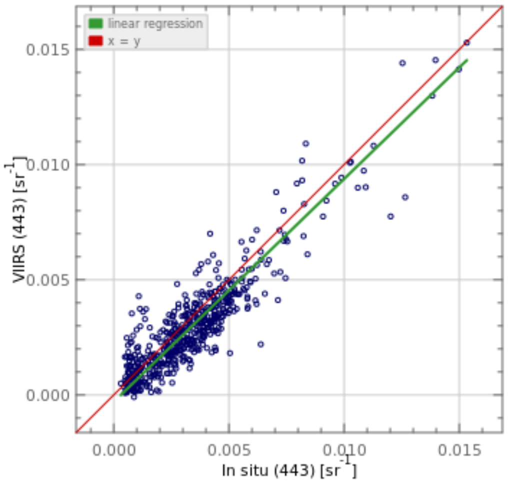

Rrs(547)

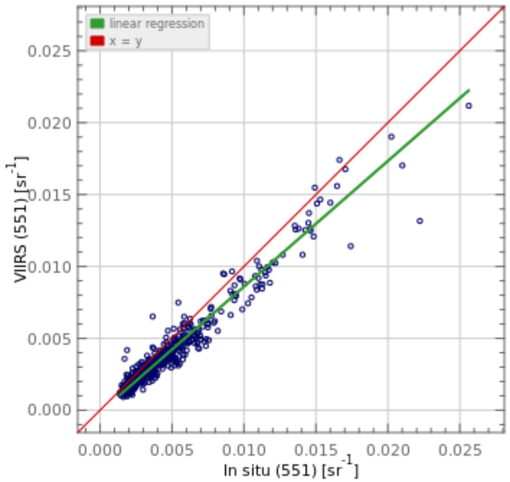

Chl_a

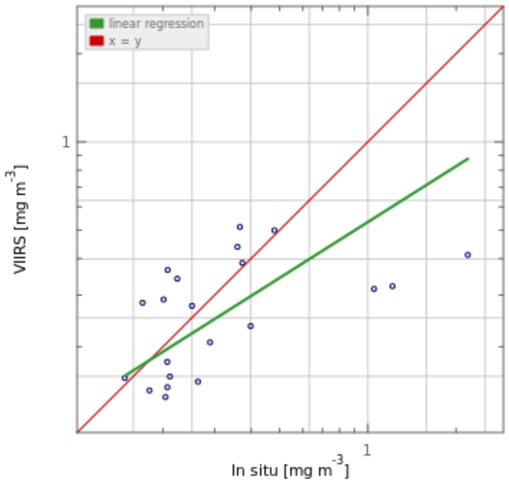

Product Name	VIIRS Range	In situ Range	#	Best Fit Slope	Best Fit Intercept	R^2	Median Ratio	Abs % Difference	RMSE
Rrs410	-0.00170, 0.01185	0.00001, 0.01273	549	0.95555	-0.00049	0.71726	0.75882	33.72388	0.00139
Rrs443	-0.00009, 0.01529	0.00031, 0.01533	551	0.96766	-0.00030	0.84769	0.85058	24.30475	0.00103
Rrs486	0.00061, 0.01924	0.00101, 0.02276	551	0.86426	-0.00018	0.93398	0.80337	21.36508	0.00120
Rrs551	0.00092, 0.02118	0.00137, 0.02562	551	0.87412	-0.00015	0.94758	0.83103	17.50243	0.00112
Rrs671	-0.00023, 0.00919	0.00001, 0.00872	549	0.95335	-0.00020	0.85823	0.72070	31.53838	0.00049

Product Name	VIIRS Range	In situ Range	#	Best Fit Slope*	Best Fit Intercept*	R^2*	Median Ratio	Abs % Difference	RMSE*
chlor_a	0.13469, 0.51238	0.14823, 2.19377	21	0.63292	-0.27375	0.51249	0.85871	33.97323	0.27166

* statistical calculations based on log10

MODISA R2013.1 In Situ Validation

Rrs(443)

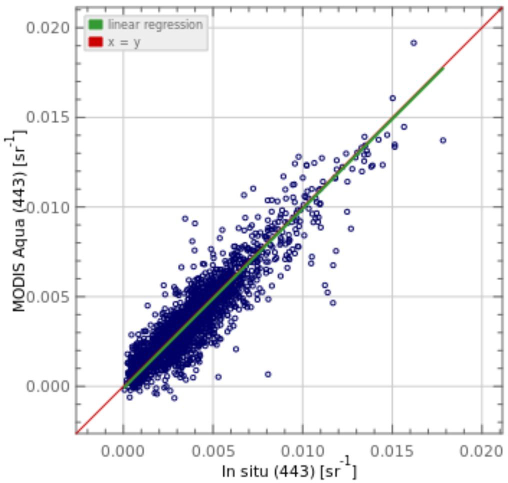

Rrs(547)

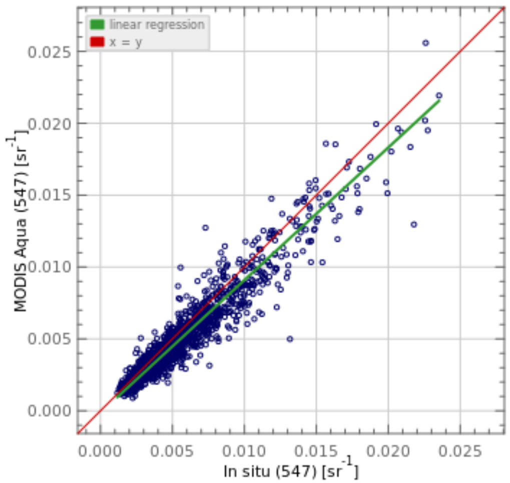

Chl_a

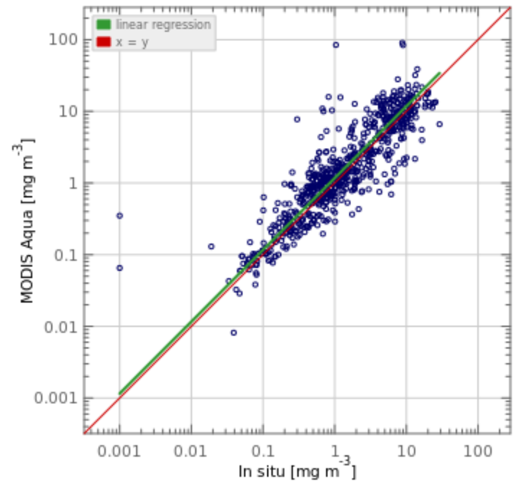

Product Name	MODIS Aqua Range	In situ Range	#	Best Fit Slope	Best Fit Intercept	R^2	Median Ratio	Abs % Difference	RMSE
Rrs412	-0.00261, 0.01820	0.00002, 0.01964	1954	0.99291	-0.00059	0.77055	0.82390	30.41368	0.00151
Rrs443	-0.00065, 0.01916	0.00007, 0.01783	2124	1.00106	-0.00011	0.85345	0.98369	16.73993	0.00105
Rrs488	0.00033, 0.02030	0.00039, 0.02289	1829	0.90079	-0.00012	0.91138	0.87838	14.98993	0.00112
Rrs531	0.00092, 0.02045	0.00133, 0.02285	724	0.91916	-0.00022	0.92451	0.87761	13.88098	0.00119
Rrs547	0.00089, 0.02559	0.00117, 0.02353	1702	0.92216	-0.00013	0.92495	0.89320	12.55173	0.00111
Rrs667	-0.00034, 0.01186	0.00001, 0.01100	1620	1.02181	-0.00019	0.87108	0.80298	28.30381	0.00041
Rrs678	-0.00034, 0.01009	0.00010, 0.00904	385	1.17917	-0.00034	0.86345	0.77994	31.52185	0.00045

Product Name	MODIS Aqua Range	In situ Range	#	Best Fit Slope*	Best Fit Intercept*	R^2*	Median Ratio	Abs % Difference	RMSE*
chlor_a	0.00818, 90.17510	0.00100, 29.00400	695	1.00199	0.06869	0.81326	1.13231	38.19472	0.32752

* statistical calculations based on log10

MODISA showing agreement with R2014.0 VIIRS

Chlorophyll (OCI) Deep-Water Time-Series

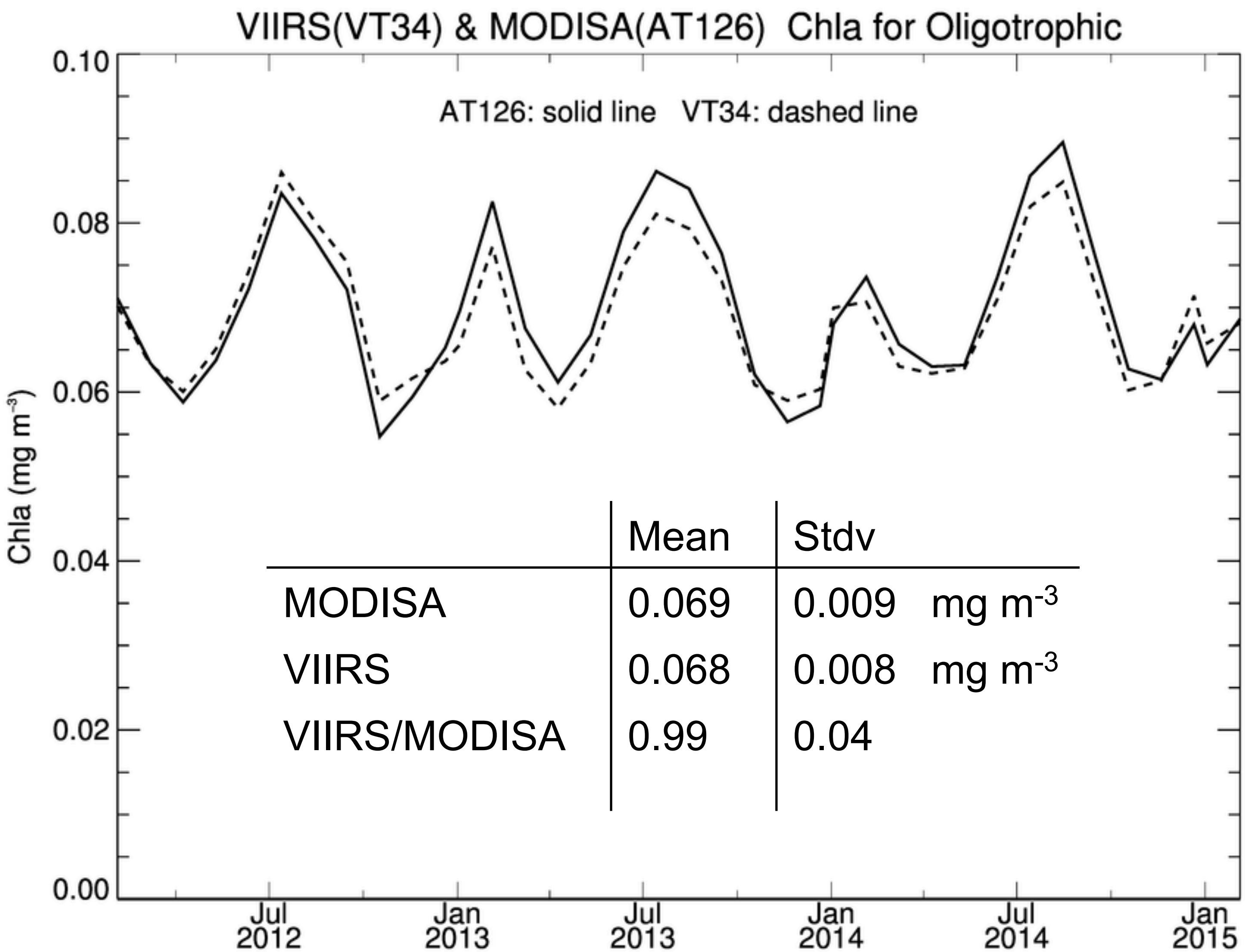

	Mean	Stdv	
MODISA	0.069	0.009	mg m^{-3}
VIIRS	0.068	0.008	mg m^{-3}
VIIRS/MODISA	0.99	0.04	

Summary

- MODIS continuity algorithm for the retrieval of Rrs and Chlorophyll (and other derived products) has been implemented for VIIRS.
- VIIRS Rrs temporal stability is much improved following extensive recalibration effort, and range of variability is now consistent with historical norms following VIIRS Reprocessing 2014.0.
- MODIS-Aqua temporal variability has increased in the blue since 2011, with a large departure in all bands in 2014. Efforts have been made to address these issues with some success.
- MODIS-Aqua and VIIRS Rrs and derived Chlorophyll are comparable in magnitude and spatial distribution, show a similar level of agreement with in situ validation, and show good temporal consistency (based on latest test results).

MODISA Reprocessing 2014.0 in progress!

Summary

- MODIS-Terra calibration updates and reprocessing will be addressed once MODIS-Aqua reprocessing is complete.

back-up

determining aerosol contribution

assume $L_w(\lambda) = 0$ at two NIR (or SWIR) bands, **or that it can be estimated with sufficient accuracy**.

retrieve aerosol reflectance in each NIR band as

known

$$\left[L_a + L_{ra}\right] = \frac{L_t}{t_{gv}\, t_{gs}\, f_p} - \left(L_r + t_{dv} L_f + T_s T_v L_g + t_{dv} L_w\right)$$

$$\rho_a = \left[L_a + L_{ra}\right] \frac{\pi}{F_0 \cos(\theta_0)}$$

use spectral dependence of retrieved NIR aerosol reflectance (ε) to select the most appropriate aerosol model from a suite of pre-computed models

use NIR aerosol reflectance and selected aerosol model to extrapolate aerosol reflectance to visible wavelengths

aerosol model tables

- vector RT code (Ahmad-Fraser)
- based on AERONET size distributions & albedos
- 80 models (10 size fractions within 8 humidities)
  - 100% coarse mode to 95% fine mode
  - non- or weakly absorbing
- LUT: extinction, albedo, phase function, ss->ms, t_d
  - function of path geometry (or scattering angle)
- model selection discriminated by relative humidity

Fine Mode Albedo

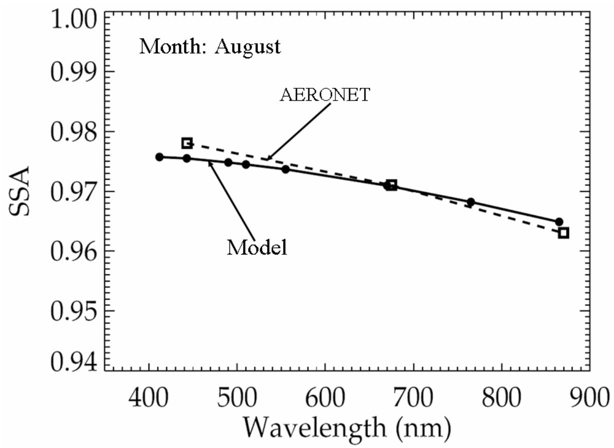

Typical Size Distributions

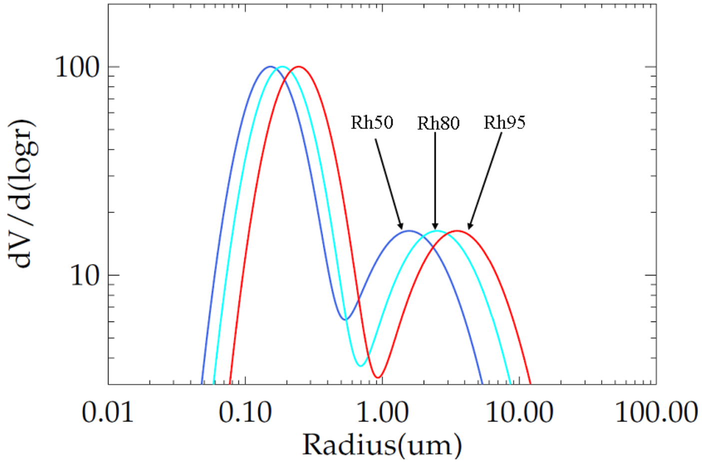

Mean AERONET Fine & Coarse Modal Radii

Rh	r_{vf}	σ_f	r_{vc}	σ_c	r_{vf}/r_{ovf}	r_{vc}/r_{ovc}
0.30	0.150	0.437	2.441	0.672	1.006	1.009
0.50	0.152	0.437	2.477	0.672	1.019	1.024
0.70	0.158	0.437	2.927	0.672	1.063	1.210
0.75	0.167	0.437	3.481	0.672	1.118	1.439
0.80	0.187	0.437	3.966	0.672	1.255	1.639
0.85	0.204	0.437	4.243	0.672	1.371	1.753
0.90	0.221	0.437	4.638	0.672	1.486	1.917
0.95	0.246	0.437	5.549	0.672	1.648	2.293

Ahmad et al. 2010, Appl. Opt.

aerosol model selection & application

select the two sets of 10 models (10 size fractions) with relative humidity (RH) that bound the RH of the observation.

find the two models that bound the observed epsilon within each RH model family.

$$\varepsilon^{obs}(748,869) = \frac{\rho_a(748)}{\rho_a(869)} \rightarrow \varepsilon^{\mathrm{mod}}(748,869)^{*}$$

use model epsilon to extrapolate to visible.

$$\rho_a(\lambda) = \rho_a(869)\varepsilon^{\mathrm{mod}}(\lambda,869)$$

compute weighted average, $\bar{\rho}_a$, between models within each RH family, and then again between bounding RH solutions.

$$[L_a + L_{ra}] = \bar{\rho}_a(\lambda)\frac{F_0\cos(\theta_0)}{\pi}$$

model epsilon

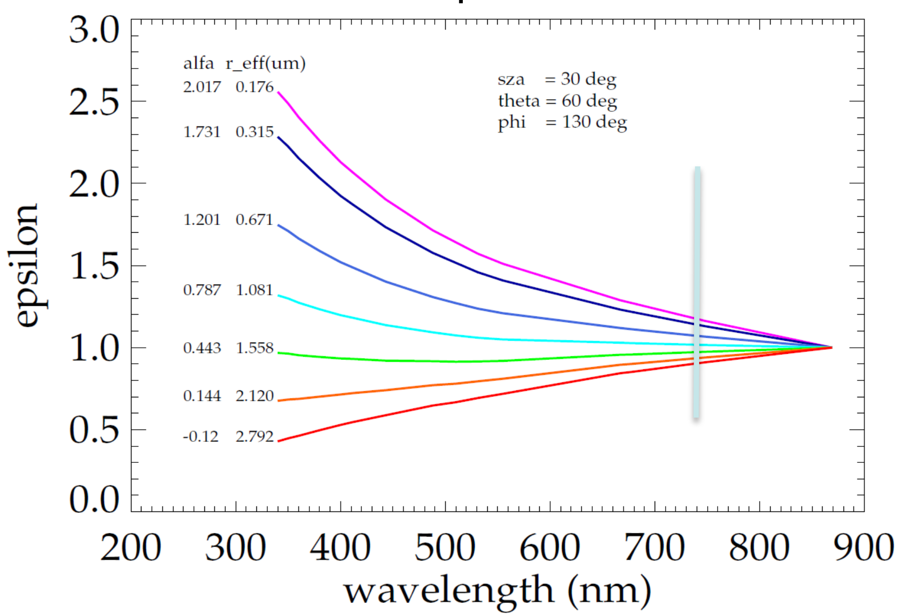

**actually done in single scattering space and transformed to multi-scattering*

we estimate $L_w(NIR)$ using a bio-optical model

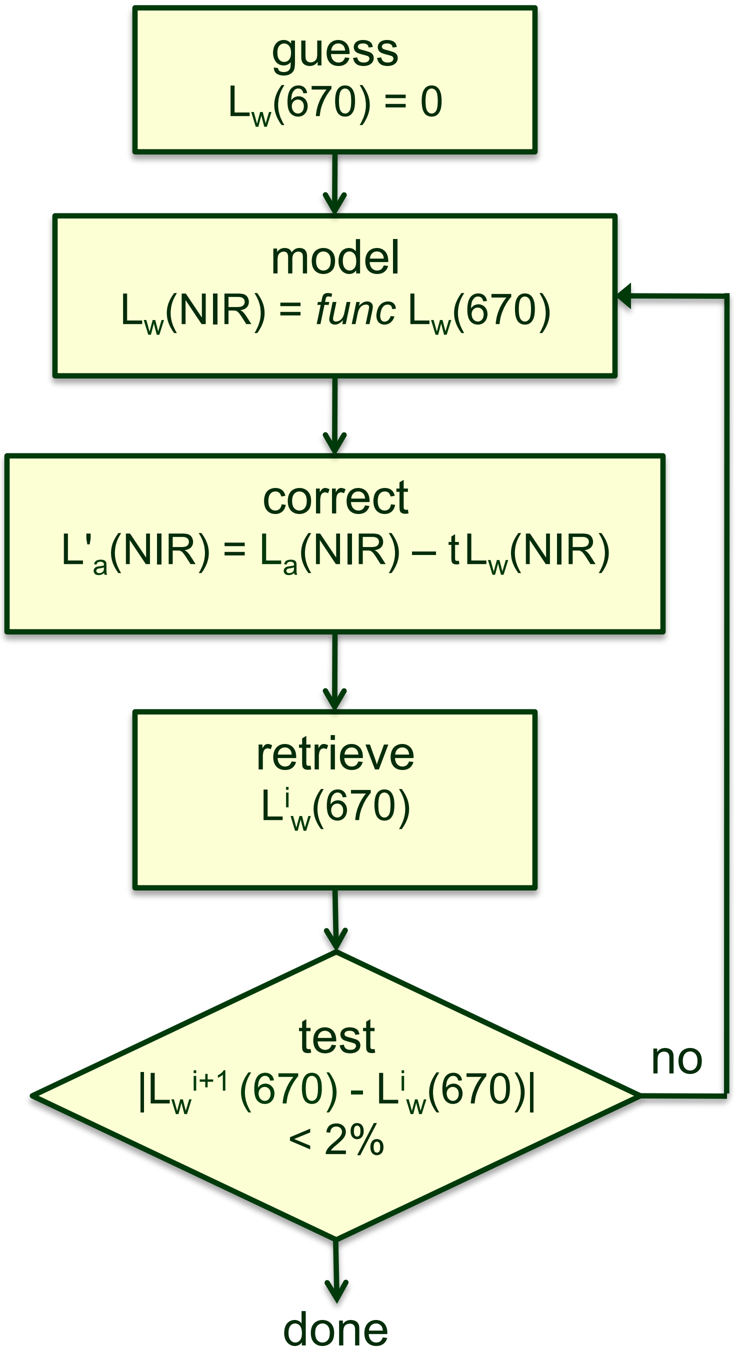

1) convert $L_w(670)$ to $b_b/(a+b_b)$

   via Morel f/Q and retrieved Chl_a

2) estimate $a(670) = a_w(670) + a_{pg}(670)$

   via NOMAD empirical relationship

$$a(670) = e^{(\ln(C_a)*0.9389-3.7589)} + a_w(670)$$

3) estimate $b_{bp}(NIR) = b_{bp}(670)\ (\lambda/670)^{\eta}$

   via Lee et al. 2002

$$\eta = 2.0 * \left[1. - 1.2 * e^{(-0.9*R_{rs}(443)/R_{rs}(555))}\right]$$

4) assume $a(NIR) = a_w(NIR)$

5) estimate $L_w(NIR)$ from $b_b/(a+b_b)$

   via Morel f/Q and retrieved Chl_a

Bailey et al., Optics Express, 2010

brdf correction

to account for shape of sub-surface light-field due to position of the Sun and optical properties of the water column.

based on pre-computed look-up tables from hydrolight simulations of Morel et al. 2002, Appl. Opt.

given radiant path geometry $(\theta_0,\theta,\Delta\varphi)$, windspeed (w) and **Chl**

Chl = f(R'$_{rs}$(λ))

$$R'_{rs} = \frac{L_w}{F_0 \cos(\theta_s) t_{ds} f_s} f_\lambda$$

$\theta_0=0,\ \theta=0, \Delta\varphi=0$

$f_b(\lambda,\theta_0,\theta,\Delta\varphi,\mathrm{Chl},w) = (\mathcal{R}_0\ f_0/Q_0)\ /\ (\mathcal{R}\ f/Q)$

f/Q relates subsurface irradiance reflectance to radiance reflectance

$\mathcal{R}$ includes all reflection/refraction effects of the air-sea interface

$R_{rs}(\lambda) = R'_{rs}(\lambda)\ f_b(\lambda,\theta_0,\theta,\Delta\varphi,\mathrm{Chl},w)$

Chl = f(R$_{rs}$(λ))

iteration

adaptation to VIIRS

- standard MODIS atmospheric correction software was modified (previous S-NPP science team) to also process VIIRS
- starts from VIIRS pseudo Level-1A (SDR with no temporal calibration), and applies instrument calibration in Level-1A to Level-2
  - pseudo Level-1A to be replaced by NASA Level-1A (when operational)
  - instrument calibration developed by OBPG (Eplee et al. 2015)
- algorithm modifications limited to adjustment for sensor-specific spectral band centers and relative spectral responses
- same Ahmad-Fraser vector radiative transfer code used to derive MODIS & VIIRS-specific Rayleigh and aerosol model tables
- bands used for aerosol determination
  - MODIS: 748 & 869 nm
  - VIIRS: 745 & 862 nm